Biol Cybern (2014) 108:85–101
DOI 10.1007/s00422-013-0582-2

ORIGINAL PAPER

Biological Cybernetics

Sensory uncertainty and stick balancing at the fingertip

Tamas Insperger · John Milton

Received: 4 October 2013 / Accepted: 20 December 2013 / Published online: 25 January 2014

Abstract The effects of sensory input uncertainty, ε, on the stability of time-delayed human motor control are investigated by calculating the minimum stick length, ℓ_{crit}, that can be stabilized in the inverted position for a given time delay, τ. Five control strategies often discussed in the context of human motor control are examined: three time-invariant controllers [proportional–derivative, proportional–derivative–acceleration (PDA), model predictive (MP) controllers] and two time-varying controllers [act-and-wait (AAW) and intermittent predictive controllers]. The uncertainties of the sensory input are modeled as a multiplicative term in the system output. Estimates based on the variability of neural spike trains and neural population responses suggest that $\varepsilon \approx 7$–$13\,\%$. It is found that for this range of uncertainty, a tapped delay-line type of MP controller is the most robust controller. In particular, this controller can stabilize inverted sticks of the length balanced by expert stick balancers (0.25–0.5 m when $\tau \approx 0.08$ s). However, a PDA controller becomes more effective when $\varepsilon > 15\,\%$. A comparison between ℓ_{crit} for human stick balancing at the fingertip and balancing on the rubberized surface of a table tennis racket suggest that friction likely plays a role in balance control. Measurements of ℓ_{crit}, τ, and a variability of the fluctuations in the vertical displacement angle, an estimate of ε, may make it possible to study the changes in control strategy as motor skill develops.

T. Insperger (✉)
Department of Applied Mechanics, Budapest University of Technology and Economics, 1521 Budapest, Hungary
e-mail: insperger@mm.bme.hu

J. Milton
W. M. Keck Science Center, Claremont Colleges, Claremont, CA 91771, USA
e-mail: jmilton@jsd.claremont.edu

Keywords Stick balancing · Feedback delay · Sensory uncertainties · Control

1 Introduction

Visually directed voluntary movements are under the control of a motor program that is modifiable by time-delayed sensory feedback (Shadmehr et al. 2010; Todorov and Jordan 2002). Investigations involving motor imagery (Milton et al. 2007; Pau et al. 2013) and brain–machine interfaces (Hochberg et al. 2012) establish that the motor plan can be generated "from thoughts alone," but that skilled task performance requires sensory feedback (Kuiken et al. 2007; Suminski et al. 2010). How is online feedback control achieved using time-delayed feedback? All time-delayed feedback controllers are predictive in the sense that information available at time t is used to predict corrective actions made at time $t + \tau$, where τ is the time delay. The unsettled question concerns whether the nervous system bases these predictions solely on sensory information collected at a single instance in time or uses an internal model obtained by solving the system equations over the delay interval.

Two types of control approaches have been considered: (1) stabilization with sensory feedback (Milton et al. 2009a; Stepan 2009) and (2) stabilization with delay compensation (Nijhawan and Wu 2009; Stanley and Miall 2009). Commonly considered sensory feedback controllers are proportional–derivative (PD) and proportional–derivative–acceleration (PDA). It is well established that such controllers cannot stabilize an inverted pendulum of a given length unless the feedback delay is smaller than a critical delay (Schurer 1948; Stepan 1989). The goal of delay compensating controllers is to take the delay out of the control loop (Krstic 2009). For example, the celebrated Smith predictor compen-

sates the delay using an internal model to predict the actual state variables of the system (Miall et al. 1993; Miall and Jackson 2006; Smith 1957). However, its practical applicability is limited by the fact that it cannot be used to stabilize an unstable open-loop system such as stick balancing and it is very sensitive to mismatch between the internal model parameters and the actual system parameters (Palmor 2000; Michiels and Niculescu 2003). Model predictive (MP) controllers overcome the limitations of the Smith predictor by solving the system equations over the delay period (Krstic 2009). Examples include controllers based on optimal control (Kleinman 1969), the finite spectrum assignment (Manitius and Olbrot 1979; Wang et al. 1998), the reduction approach (Arstein 1982) and the modified Smith predictor (Palmor 2000). However, MP controllers are sensitive to implementation inaccuracies and to parameter estimation uncertainties (Engelborghs et al. 2001; Mondié et al. 2002).

An alternate approach for delay compensation is the use of intermittent controllers in which the feedback is intermittently turned on and off. For an act-and-wait (AAW) controller, the delay can be eliminated if the switch-off (waiting) period is longer than the feedback delay (Insperger 2006; Insperger and Stepan 2011). Another type of time-varying controllers is the intermittent predictive (IP) controller (Gawthrop and Wang 2007), which makes use of open-loop control intervals with a system-matched hold in order to get a simplified prediction over the delay period. IP control provides a simpler algorithm than its continuous counterpart, while it explains a wide range of experiments (Gawthrop et al. 2011).

There are a number of characteristics that distinguish the performance of task specific, goal-directed voluntary motor skills from movements controlled by neural reflexes or central pattern generators. The most striking differences are the relationships between practice and skill. Practice, often ranging over weeks to years, is required to both attain and maintain a given skill level. Some individuals are unable to become skilled even with considerable practice, whereas under appropriately stressful conditions, skill levels can rapidly deteriorate ["choking" (Beilock 2011)]. In the context of mathematical models of motor control, the practice dependence of skill levels is most often interpreted in terms of a learning-dependent optimization of the important control parameters, e.g., gains, in the proposed controller. For example, it is well established that inaccuracies can be reduced by a learning process through a feedback error-learning scheme (Kawato 1990; Gomi and Kawato 1993; Valero-Cuevas et al. 2009). However, uncertainty in the input signal is likely to be independent of skill levels since it is a function of the properties of sensory receptors and disturbances from the environment. Although it is increasingly being recognized that noise plays an important role in the nervous system (McDonnell and Ward 2011), especially when time delays are present (Milton 2011), little work has appeared on the behavior of time-delayed feedback control schemes in the face of uncertain sensory inputs.

In this paper, we examine the effects of input uncertainty on the ability of five different control concepts to stabilize an inverted pendulum: PD, PDA, MP, AAW and IP. These comparisons are based on the observation that if the time delay is known, then the shortest stick length that can be stabilized by a given controller can be calculated. The sensory uncertainty is modeled as a multiplicative term in the system output. We find that although the stability of each controller has different sensitivities to input uncertainty, in all cases, uncertainty levels of just a few percent can result in the loss of stability. Since the stabilization of an inverted pendulum is an important benchmark of control systems theory (Milton et al. 2009a), we anticipate that our observations are not limited to problems related to balance control.

The paper is outlined as follows. First, in Sect. 2, the important aspects of the control of an inverted pendulum are reviewed. Section 3 shows how uncertainty is introduced into these models with sampled output. In Sect. 4, the sensitivity of the stability of the PD, PDA, MP, AAW and IP controllers to sensory uncertainties is examined, and then in Sect. 5, we show how input uncertainty affects the shortest stick length that can be balanced for a given delay. Section 6 deals with the effect of sampling on the balancing process. Finally, the importance of our observations for developing models of voluntary model control is discussed.

2 Stick balancing model

A schematic model for stick balancing at the finger tip is shown in Fig. 1. It is assumed that the bottom point of the stick can freely move both in the horizontal and in the vertical directions; thus, the system is a 3 degree-of-freedom system. The general coordinates can be chosen as the horizontal and the vertical displacements of the stick's bottom point denoted by x and y and the angular position of the stick denoted by φ. The feedback control forces, Q_x and Q_y, keep the stick

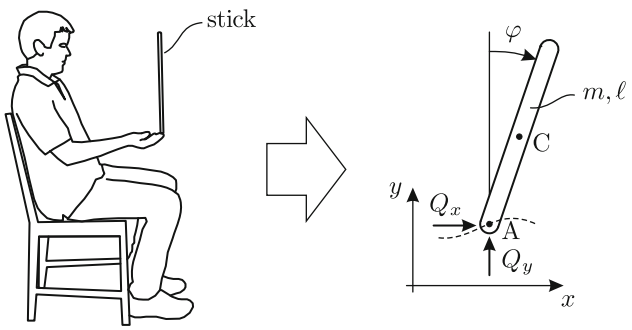

Fig. 1 Sketch and mechanical model of stick balancing

at the position $(x, y, \varphi) = (0, 0, 0)$. Our goal is to determine for a given τ, the shortest stick, ℓ_{crit} that can be stabilized for different choices of Q_x and Q_y.

This stick balancing problem can be reduced to a one-degree-of-freedom system described by

$$J_C\ddot{\varphi}(t) - mgc\varphi(t) = -Q_x^{\text{fb}}(t)c, \tag{1}$$

where m is the mass of the stick, c is the distance between the bottom (A) and the center of gravity (C) of the stick, J_C is the moment of inertia with respect to the normal line via the center of gravity, and Q_x^{fb} is the feedback control force in the horizontal (x) direction. We assume that the stick is homogeneous, thus $c = \ell/2$ and $J_C = m\ell^2/12$, where ℓ is the length of the stick and Eq. (1) becomes

$$\ddot{\varphi}(t) - a\varphi(t) = -u(t), \tag{2}$$

where $a = 6g/\ell$ is the system parameter, and $u(t) = 6\,Q_x^{\text{fb}}(t)/m\ell$ is the input. The first-order representation of the system is

$$\dot{\mathbf{x}}(t) = \mathbf{A}\mathbf{x}(t) + \mathbf{B}u(t), \tag{3}$$

where

$$\mathbf{x}(t) = \begin{pmatrix} \varphi(t) \\ \dot{\varphi}(t) \end{pmatrix}, \quad \mathbf{A} = \begin{pmatrix} 0 & 1 \\ a & 0 \end{pmatrix} \quad \text{and} \quad \mathbf{B} = \begin{pmatrix} 0 \\ -1 \end{pmatrix} \tag{4}$$

are the state vector, the system matrix and the input matrix, respectively.

Equation (1) is obtained from the equations of motion

$$m\ddot{x}(t) + mc\ddot{\varphi}(t)\cos(\varphi(t)) - mc\dot{\varphi}^2(t)\sin(\varphi(t)) = Q_x(t), \tag{5}$$

$$m\ddot{y}(t) - mc\ddot{\varphi}(t)\sin(\varphi(t)) - mc\dot{\varphi}(t)^2\cos(\varphi(t)) = Q_y(t) - mg, \tag{6}$$

$$J_C\ddot{\varphi}(t) = Q_y(t)c\sin(\varphi(t)) - Q_x(t)c\cos(\varphi(t)). \tag{7}$$

In general, the control forces can be resolved into feedforward and feedback components as

$$Q_x(t) = Q_x^{\text{ff}}(t) + Q_x^{\text{fb}}(t), \tag{8}$$

$$Q_y(t) = Q_y^{\text{ff}}(t) + Q_y^{\text{fb}}(t), \tag{9}$$

where $Q_x^{\text{ff}}(t)$ and $Q_y^{\text{ff}}(t)$ are the feedforward terms and $Q_x^{\text{fb}}(t)$ and $Q_y^{\text{fb}}(t)$ are the feedback terms (Abed et al. 2000). The feedforward terms are determined by the inverse dynamics (Jordan 1996; Kawato 1999): substitution of $(x, y, \varphi) = (0, 0, 0)$ into Eqs. (5)–(7) gives $Q_x^{\text{ff}}(t) = 0$ and $Q_y^{\text{ff}}(t) = mg$. Note, however, that if the feedforward component contains a predefined time-dependent term $f(t)$ such as

$$Q_y^{\text{ff}}(t) = mg + f(t), \tag{10}$$

then it appears as a parametric excitation (i.e., time-dependent coefficient) in the linearized equation as

$$J_C\ddot{\varphi}(t) - (mg + f(t))c\varphi(t) = -Q_x^{\text{fb}}(t)c. \tag{11}$$

Although parametric excitation may contribute to the stabilization of the stick in case of a continuous periodic excitation (Milton et al. 2009b; Insperger 2011), it is a feedforward stabilization and not a feedback mechanism. Thus, we do not consider parametric excitation further.

Linearization of Eqs. (5)–(7) around the equilibrium $(x, y, \varphi) = (0, 0, 0)$ and $(Q_x, Q_y) = (Q_x^{\text{ff}}, Q_y^{\text{ff}})$ gives

$$m\ddot{x}(t) + mc\ddot{\varphi}(t) = Q_x^{\text{fb}}(t), \tag{12}$$

$$m\ddot{y}(t) = Q_y^{\text{fb}}(t), \tag{13}$$

$$J_C\ddot{\varphi}(t) - mgc\varphi(t) = -Q_x^{\text{fb}}(t)c, \tag{14}$$

Note that Eqs. (1) and (14) are the same. It can be seen that Eq. (13) can be separated from Eqs. (12) and (14). This means that the vertical position y is not controllable through the horizontal feedback force $Q_x^{\text{fb}}(t)$, while the horizontal position x and the angular displacement φ are not controllable through the vertical feedback force $Q_y^{\text{fb}}(t)$. Thus, one can conclude that the feedback control force $Q_y^{\text{fb}}(t)$ in the vertical direction does not affect the linear stability of the stick at the vertical equilibrium.

Equations (12) and (14) govern the horizontal and the angular displacement of the stick, while Eq. (13) governs the vertical displacement. The characteristic roots (poles) of the open-loop system [i.e., Eqs. (12), (13) and (14) with $Q_x^{\text{fb}}(t) = 0$ and $Q_y^{\text{fb}}(t) = 0$] are $\lambda_{1,2,3,4} = 0$ and $\lambda_{5,6} = \pm\sqrt{mgc/J_c}$. The roots $\lambda_{1,2,3,4} = 0$ correspond to the horizontal and the vertical position of the stick's bottom. This means that the point $(x, y) \equiv (0, 0)$ is a marginally stable equilibrium of the subspace $(x, y, \dot{x}, \dot{y})$. The roots $\lambda_{5,6} = \pm\sqrt{mgc/J_c}$ correspond to the angular displacement of the stick and show that the vertical position $\varphi = 0$ is unstable since $\text{Re}(\lambda_6) = -\sqrt{mgc/J_c} < 0$.

These observations imply that the horizontal and the vertical positions of the stick are asymptotically stable even for a feedback with very small control gains. Thus, the important control problem is the stabilization of the angular displacement since it is associated with the unstable characteristic root $\lambda_6 = -\sqrt{mgc/J_c}$. This observation emphasizes the importance of Eq. (1). For example, the feedback law

$$Q_x^{\text{fb}}(t) = -k_{\text{p}1}x(t) - k_{\text{p}3}\varphi(t) - k_{\text{d}1}\dot{x}(t) - k_{\text{d}3}\dot{\varphi}(t), \tag{15}$$

$$Q_y^{\text{fb}}(t) = -k_{\text{p}2}y(t) - k_{\text{d}2}\dot{y}(t) \tag{16}$$

can stabilize the vertical and the horizontal displacement of the stick's bottom for any $k_{\text{p}1} > 0$, $k_{\text{p}2} > 0$, $k_{\text{d}1} > 0$ and $k_{\text{d}2} > 0$, while the stabilization of the angular position requires a careful tuning of $k_{\text{p}3}$ and $k_{\text{d}3}$ (with respect to $k_{\text{p}1}$

and k_{d1}). Here, k_{pi}, k_{di} $(i = 1, 2, 3)$ are the proportional and the derivative control gains for x, y and φ, respectively.

3 Modeling uncertainties in delayed motor control systems

The feedback delay appears in the control law such that the actual input depends on delayed values of the state. For instance, the control force in case of a continuous-time-delayed PD controller reads

$$Q_x^{\mathrm{fb}}(t) = K_{\mathrm{p}}\varphi_{\mathrm{s}}(t-\tau) + K_{\mathrm{d}}\dot{\varphi}_{\mathrm{s}}(t-\tau), \tag{17}$$

where K_{p} and K_{d} are the proportional, and the derivative control gains, and $\varphi_{\mathrm{s}}(t)$ and $\dot{\varphi}_{\mathrm{s}}(t)$ are the angular position and angular velocity perceived by the sensory system. The observation that stick balancing is much less successful with eyes closed suggests that vision plays a dominant role, but does not exclude roles for other sensory inputs such as those from cutaneous mechanoreceptors. Indeed, the measured τ is longer when cutaneous mechanoreceptor input is diminished, e.g., stick balancing (3D) on a table tennis racket [0.22 s (Mehta and Schaal 2002)] and virtual stick balancing (2D) [0.25–0.4 s (Cabrera et al. 2004; Patzelt and Pawelzik 2011)], than observed for stick balancing at the fingertip [∼0.08 s (Cabrera and Milton 2004)]. In Sect. 4, we illustrate our findings using $\tau = 0.1$ s, and in Sect. 5, we compare ℓ_{crit} obtained for this delay to those obtained for other choices of τ.

Motor control is most often modeled as a discrete-time system or, what is equivalent, a continuous-time feedback system with sampled output (Jordan 1996; Todorov and Jordan 2002; Mehta and Schaal 2002). Here, we assume that the state and the efferent copies are available only at discrete-time instants $t_i = i\Delta t$, $i = 1, 2, \ldots$, where Δt is the sampling period, and that the feedback delay is integer multiple of the sampling period, i.e., $\tau = r\Delta t$, where integer r is called discrete delay. In the case of a PD controller with zero-order hold, the corresponding control force [the sampled output piecewise-constant counterpart of Eq. (17)] is

$$Q_x^{\mathrm{fb}}(t) = K_{\mathrm{p}}\varphi_{\mathrm{s}}(t_{i-r}) + K_{\mathrm{d}}\dot{\varphi}_{\mathrm{s}}(t_{i-r}), \quad t \in [t_i, t_{i+1}). \tag{18}$$

We assume a sampling period $\Delta t = 10$ ms, which implies that the discrete delay is $r = 10$ when $\tau = 100$ ms. For comparison, Mehta and Schaal (2002) used a 60-Hz sampling frequency, which corresponds to $\Delta t = 16.67$ ms.

In order to describe sensory input uncertainties, we introduce the uncertainty radius as the maximum specific difference between the actual and the perceived values of the state variables. Specifically, we introduce the sensory input uncertainty as a multiplicative term in the system output. The sensory uncertainty radius for the angular position is denoted by ε_{p}. We assume that the angular position perceived by the sensory system can be given as $\varphi_{\mathrm{s}}(t) = (1 + \delta_{\mathrm{p}})\varphi(t)$, where $\varphi(t)$ is the actual angular position, and δ_{p} is an uncertainty parameter such that $|\delta_{\mathrm{p}}| \leq \varepsilon_{\mathrm{p}}$. The uncertainty radii for the angular velocity (ε_{v}), the angular acceleration (ε_{a}) and the efferent copies of the control commands (ε_{u}) can be defined in a similar fashion. The stability of the system will be analyzed with respect to the sensory uncertainty radii. The concept of this analysis is similar to the stability radius with respect to changes in the system parameters (Michiels and Roose 2003; Michiels and Niculescu 2007).

4 Different control concepts

In this section, we determine the conditions for stabilizing the upright position of a stick balanced at the fingertip for five different linear control models that commonly arise in the setting of motor control: PD, PDA, MP, AAW and IP. All of these controllers are analyzed for the system described by Eq. (3) with (4). In order to facilitate comparison between the different control models, we compute the stability diagrams as a function of uncertainty for a stick of length 1 m and a time delay of 100 ms. The sampled output vector is given as

$$\mathbf{y}(t_i) = \begin{pmatrix} \varphi_{\mathrm{s}}(t_i) \\ \dot{\varphi}_{\mathrm{s}}(t_i) \end{pmatrix}, \tag{19}$$

where $\varphi_{\mathrm{s}}(t_i)$ and $\dot{\varphi}_{\mathrm{s}}(t_i)$ are the angular position and angular velocity perceived by the sensory system at time instant $t_i = i\Delta t$. Sensory uncertainties are introduced using an output matrix

$$\mathbf{C} = \begin{pmatrix} 1+\delta_{\mathrm{p}} & 0 \\ 0 & 1+\delta_{\mathrm{v}} \end{pmatrix}, \tag{20}$$

where $|\delta_{\mathrm{p}}| \leq \varepsilon_{\mathrm{p}}$ and $|\delta_{\mathrm{v}}| \leq \varepsilon_{\mathrm{v}}$ with ε_{p} and ε_{v} being the sensory uncertainty radii for the angular position and for the angular velocity according to Sect. 3. The output is then given as

$$\mathbf{y}(t_i) = \mathbf{C}\mathbf{x}(t_i). \tag{21}$$

We will also use the control matrix

$$\mathbf{K} = \begin{pmatrix} k_{\mathrm{p}} & k_{\mathrm{d}} \end{pmatrix}, \tag{22}$$

where $k_{\mathrm{p}} = 6K_{\mathrm{p}}/(m\ell)$ and $k_{\mathrm{d}} = 6K_{\mathrm{d}}/(m\ell)$.

4.1 Proportional–derivative (PD) control

The governing equations for PD control take the form of a retarded functional differential equation (RFDE). Although

RFDEs have infinitely many roots, only finitely many of them can have positive real parts leading to instability (Hale and Lunel 1993; Stepan 1989). The stability criteria for continuous-time-delayed PD feedback

$$\ddot{\varphi}(t) - a\varphi(t) = -k_\mathrm{p}\varphi(t-\tau_\mathrm{p}) - k_\mathrm{d}\dot{\varphi}(t-\tau_\mathrm{d}) \tag{23}$$

have been extensively studied for the cases when $\tau_\mathrm{d} \neq 0$ (Milton et al. 2009a; Stepan 1989) and when $\tau_\mathrm{d} = 0$ (Cabrera and Milton 2002). When $\tau_\mathrm{p} = \tau_\mathrm{d} = \tau \neq 0$, the upright position will be unstable if the system parameter a is larger than a critical value given by

$$a_{\mathrm{crit,PD,cont}} = \frac{2}{\tau^2}, \tag{24}$$

for any k_p and k_d (Schurer 1948; Insperger and Stepan 2011). Consequently, the critical stick length is

$$\ell_{\mathrm{crit,PD,cont}} = \frac{6g}{a_{\mathrm{crit,PD,cont}}} = 3g\tau^2. \tag{25}$$

Thus, for example, if $\tau = 100\,\mathrm{ms}$, then a stick shorter than 29.4 cm cannot be balanced.

If the sampling effect with a zero-order hold is involved into the model, then the system is described by

$$\ddot{\varphi}(t) - a\varphi(t) = -k_\mathrm{p}\varphi(t_{i-r}) - k_\mathrm{d}\dot{\varphi}(t_{i-r}), \quad t \in [t_i, t_{i+1}). \tag{26}$$

For this hybrid system, the critical system parameter for the stabilizability can be given as

$$a_{\mathrm{crit,PD,disc}} = \frac{1}{\Delta t^2}\left(\ln\left(1 + \frac{1+\sqrt{2r(r+1)+1}}{r(r+1)}\right)\right)^2, \tag{27}$$

[see Enikov and Stepan (1998) for the case $r = 1$ and Insperger and Stepan (2007) for the general case $r \geq 1$]. It can be shown that $a_{\mathrm{crit,PD,disc}} < a_{\mathrm{crit,PD,cont}}$ for all finite r, that is, the sampling effect with the zero-order hold impairs stabilizability. The critical length corresponding to $\Delta t = 10$ ms and $r = 10$ is

$$\ell_{\mathrm{crit,PD,disc}} = \frac{6g}{a_{\mathrm{crit,PD,disc}}} = 32.4\,\mathrm{cm}. \tag{28}$$

Note that if $\Delta t \to 0$ and $r \to \infty$ such that $r\Delta t = \tau$, then $a_{\mathrm{crit,PD,disc}} \to a_{\mathrm{crit,PD,cont}}$ and, consequently, $\ell_{\mathrm{crit,PD,disc}} \to \ell_{\mathrm{crit,PD,cont}}$.

When sensory uncertainties are present, the control force with sampled output is given by Eq. (18). The control law associated with Eq. (3) is

$$u(t) = \mathbf{K}\mathbf{y}(t_{i-r}), \quad t \in [t_i, t_{i+1}), \tag{29}$$

where the control matrix $\mathbf{K}$ is given in Eq. (22). The system defined by Eqs. (3), (21) and (29) can be rewritten as

$$\dot{\mathbf{x}}(t) = \mathbf{A}\mathbf{x}(t) + \mathbf{B}v(t_{i-r}), \quad t \in [t_i, t_{i+1}), \tag{30}$$

$$v(t_i) = \mathbf{K}\mathbf{C}\mathbf{x}(t_i) \tag{31}$$

with $v(t_{i-r}) = u(t_i)$. Solving this system over the sampling period (t_i, t_{i+1}) gives

$$\mathbf{x}(t_{i+1}) = \mathbf{P}\mathbf{x}(t_i) + \mathbf{R}v(t_{i-r}), \tag{32}$$

where

$$\mathbf{P} = \mathrm{e}^{\mathbf{A}\Delta t}, \quad \mathbf{R} = \int_0^{\Delta t} \mathrm{e}^{\mathbf{A}(\Delta t - s)}\mathrm{d}s\,\mathbf{B}. \tag{33}$$

Equations (32) and (31) define the $(r+2)$-dimensional discrete map

$$\mathbf{z}_{i+1} = \boldsymbol{\Phi}\,\mathbf{z}_i \tag{34}$$

with

$$\mathbf{z}_i = \begin{pmatrix} \varphi(t_i) \\ \dot{\varphi}(t_i) \\ v(t_{i-1}) \\ v(t_{i-2}) \\ \vdots \\ v(t_{i-r}) \end{pmatrix}, \quad \boldsymbol{\Phi} = \begin{pmatrix} P_{11} & P_{12} & 0 & \dots & 0 & R_{11} \\ P_{21} & P_{22} & 0 & \dots & 0 & R_{21} \\ H_{11} & H_{12} & 0 & \dots & 0 & 0 \\ 0 & 0 & 1 & & 0 & 0 \\ \vdots & \vdots & & \ddots & & \vdots \\ 0 & 0 & 0 & & 1 & 0 \end{pmatrix}, \tag{35}$$

where P_{ij}, R_{ij} and H_{ij} $(i, j = 1, 2)$ denotes the corresponding elements of matrices $\mathbf{P}$, $\mathbf{R}$ and $\mathbf{H} = \mathbf{K}\mathbf{C}$. Actually, $H_{11} = k_\mathrm{p}(1+\delta_\mathrm{p})$ and $H_{12} = k_\mathrm{d}(1+\delta_\mathrm{v})$. The stability of the system can be obtained by the analysis of the eigenvalues of the coefficient matrix $\boldsymbol{\Phi}$: if all the eigenvalues are modulus less than one, then the system is asymptotically stable. The stability of the system for different uncertainty radii can be obtained by the same calculation by sweeping the uncertainty parameters δ_p and δ_p over the intervals $\delta_\mathrm{p} \in [-\varepsilon_\mathrm{p}, \varepsilon_\mathrm{p}]$ and $\delta_\mathrm{v} \in [-\varepsilon_\mathrm{v}, \varepsilon_\mathrm{v}]$.

The stability diagram is shown in Fig. 2. This stability diagram was constructed by point-by-point evaluation of the critical eigenvalues of $\boldsymbol{\Phi}$ over a fixed-sized grid of parameters K_p and K_d. If a parameter point $(K_\mathrm{p}, K_\mathrm{d})$ was found to be stable for $\delta_\mathrm{p} = 0$ and $\delta_\mathrm{v} = 0$, then it was investigated for different combinations of the uncertainty parameters $\delta_\mathrm{p} \in \{-\varepsilon_\mathrm{p}, 0, \varepsilon_\mathrm{p}\}$ and $\delta_\mathrm{v} \in \{-\varepsilon_\mathrm{v}, 0, \varepsilon_\mathrm{v}\}$ for larger and larger uncertainty radii ε_p and ε_v. For the sake of simplicity, equal uncertainty radii were assumed for the position and the velocity sensation (i.e., $\varepsilon_\mathrm{p} = \varepsilon_\mathrm{v} = \varepsilon$). For instance, the

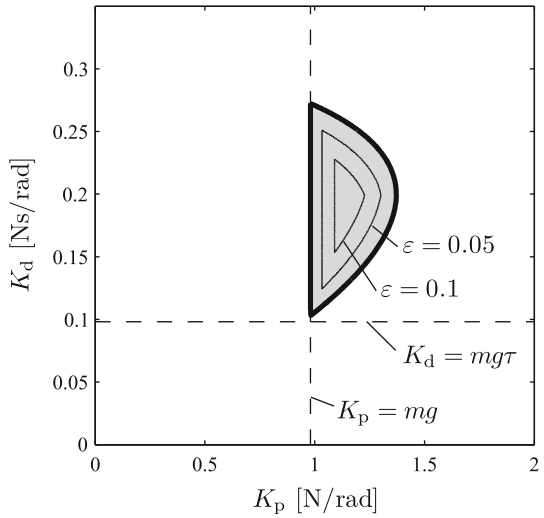

Fig. 2 Stability diagrams for the PD controller with $\Delta t = 10$ ms, $r = 10$, $\ell = 1$ m, $m = 0.1$ kg. The stable domain for zero uncertainty is indicated by *gray shading*, while the stability boundaries associated with different uncertainty radii $\varepsilon = \varepsilon_p = \varepsilon_v$ are denoted by *thin lines*

points within the contour curve $\varepsilon = 0.05$ are associated with a controller that is stable up to 5 % perturbation in the sensory inputs (i.e., in φ and $\dot{\varphi}$). It can be seen that as the uncertainty radius increases, the stable domain shrinks. No stable points were found for the uncertainty radii $\varepsilon = 0.15$. This means that a stick of length 1 m cannot be balanced by a PD controller if the uncertainty in the perception of the angular position and the angular velocity is larger than 15 %. Note that the stable parameters show up in the domain $K_p > mg$ and $K_d > mg\tau$ (Schurer 1948; Insperger and Stepan 2011). This feature will be utilized later when stabilizability conditions will be analyzed numerically.

4.2 Proportional–derivative–acceleration (PDA) control

The governing equation for PDA control is a neutral functional differential equation (NFDE). This terminology means that the delay is present in the argument of the highest derivative, namely the acceleration. In contrast to a RFDE, a NFDE can have infinitely many roots with positive real part. The stability conditions for continuous-time-delayed PDA feedback

$$\ddot{\varphi}(t) - a\varphi(t) = -k_p\varphi(t-\tau) - k_d\dot{\varphi}(t-\tau) - k_a\ddot{\varphi}(t-\tau) \quad (36)$$

have been investigated (Sieber and Krauskopf 2005; Insperger et al. 2013). It is known that if $|k_a| > 1$, then Eq. (36) is unstable with infinitely many characteristic roots with positive real parts (see Lemma 3.9 on page 63 in Stepan 1989); therefore, a necessary criteria for the stability of Eq. (36) is that $|k_a| < 1$. The critical system parameter that limits stabilizability is

$$a_{\mathrm{crit,PDA,cont}} = \frac{4}{\tau^2}. \quad (37)$$

If the system parameter a is larger than $a_{\mathrm{crit,PDA,cont}}$, then the system is unstable for any k_p, k_d and k_a. Thus, if the feedback delay is $\tau = 100$ ms, the critical length is

$$\ell_{\mathrm{crit,PDA,cont}} = \frac{6g}{a_{\mathrm{crit,PDA,cont}}} = \frac{3g\tau^2}{2} = 14.7\,\mathrm{cm}. \quad (38)$$

When sensory uncertainties are present, the control force with sampled output becomes

$$Q_x^{\mathrm{fb}}(t) = K_p\varphi_s(t_{i-r}) + K_d\dot{\varphi}_s(t_{i-r}) + K_a\ddot{\varphi}_s(t_{i-r}), \quad t \in [t_i, t_{i+1}), \quad (39)$$

where K_p, K_d and K_a are, respectively, the proportional, the derivative and the acceleration control gains, $\varphi_s(t) = (1+\delta_p)\varphi(t)$, $\dot{\varphi}_s(t) = (1+\delta_v)\dot{\varphi}(t_{i-r})$ and $\ddot{\varphi}_s(t) = (1+\delta_a)\ddot{\varphi}(t_{i-r})$ are the perceived angular position, angular velocity and angular acceleration. The sensory uncertainties are described by $|\delta_p| \le \varepsilon_p$, $|\delta_v| \le \varepsilon_v$ and $|\delta_a| \le \varepsilon_a$ with ε_p, ε_v and ε_a being the sensory uncertainty radii for the angular position, for the angular velocity and for the angular acceleration. The system output vector and the control law associated with Eq. (3) can be given as

$$\tilde{\mathbf{y}}(t_i) = \tilde{\mathbf{C}}\tilde{\mathbf{x}}(t_i), \quad t_i = i\Delta t, \quad (40)$$

$$u(t) = \tilde{\mathbf{K}}\tilde{\mathbf{y}}(t_{i-r}), \quad t \in [t_i, t_{i+1}), \quad (41)$$

where

$$\tilde{\mathbf{x}}(t) = \begin{pmatrix} \varphi(t) \\ \dot{\varphi}(t) \\ \ddot{\varphi}(t) \end{pmatrix}, \quad \tilde{\mathbf{C}} = \begin{pmatrix} 1+\delta_p & 0 & 0 \\ 0 & 1+\delta_v & 0 \\ 0 & 0 & 1+\delta_a \end{pmatrix} \quad (42)$$

and $\tilde{\mathbf{K}} = \begin{pmatrix} k_p & k_d & k_a \end{pmatrix}$ with $k_p = 6K_p/(m\ell)$, $k_d = 6K_d/(m\ell)$ and $k_a = 6K_a/(m\ell)$. Here, the output is extended by the perceived angular acceleration $\ddot{\varphi}_s(t)$.

The system defined by Eqs. (3), (40) and (41) can be rewritten as

$$\dot{\mathbf{x}}(t) = \mathbf{A}\mathbf{x}(t) + \mathbf{B}v(t_{i-r}), \quad t \in [t_i, t_{i+1}), \quad (43)$$

$$v(t_i) = \tilde{\mathbf{K}}\tilde{\mathbf{C}}\tilde{\mathbf{x}}(t_i) \quad (44)$$

with $v(t_{i-r}) = u(t_i)$. The state and its derivative at $t = t_{i+1}$ can be given as

$$\mathbf{x}(t_{i+1}) = \mathbf{P}\mathbf{x}(t_i) + \mathbf{R}v(t_{i-r}), \quad (45)$$

$$\dot{\mathbf{x}}(t_{i+1}) = \mathbf{A}\mathbf{P}\mathbf{x}(t_i) + (\mathbf{A}\mathbf{R} + \mathbf{B})v(t_{i-r}), \quad (46)$$

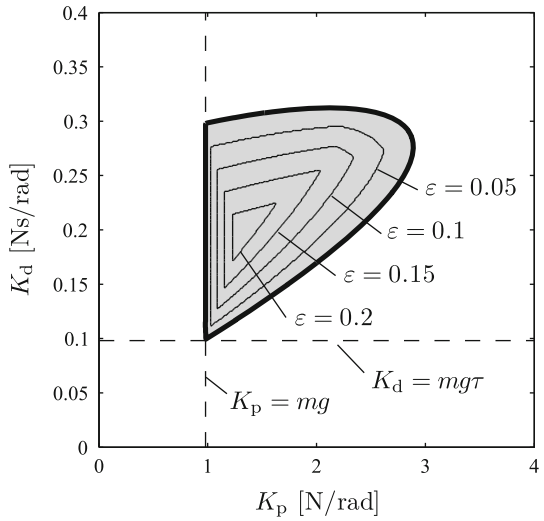

Fig. 3 Stability diagrams for the PDA controller with $\Delta t = 10$ ms, $r = 10$, $\ell = 1$ m, $m = 0.1$ kg, $K_\mathrm{a} = 0.0125$ Nms^2/rad ($k_\mathrm{a} = 0.75$). The stable domain for zero uncertainty is indicated by *gray shading*, while the stability boundaries associated with different uncertainty radii $\varepsilon = \varepsilon_\mathrm{p} = \varepsilon_\mathrm{v} = \varepsilon_\mathrm{a}$ are denoted by *thin lines*

where $\mathbf{P}$ and $\mathbf{R}$ are given in Eq. (33). The angular acceleration at $t = t_{i+1}$ is given by

$$\ddot{\varphi}(t_{i+1}) = \mathbf{Q}\mathbf{x}(t_i) + Sv(t_{i-r}), \tag{47}$$

where $\mathbf{Q} = \mathbf{DAP}$, $S = \mathbf{D}(\mathbf{AR} + \mathbf{B})$ and $\mathbf{D} = \begin{pmatrix}0 & 1\end{pmatrix}$. Equations (45), (47) and (44) define the $(r+3)$-dimensional discrete map

$$\mathbf{z}_{i+1} = \mathbf{\Phi}\mathbf{z}_i \tag{48}$$

with

$$\mathbf{z}_i = \begin{pmatrix} \varphi(t_i) \\ \dot{\varphi}(t_i) \\ \ddot{\varphi}(t_i) \\ v(t_{i-1}) \\ v(t_{i-2}) \\ \vdots \\ v(t_{i-r}) \end{pmatrix}, \quad \mathbf{\Phi} = \begin{pmatrix} P_{11} & P_{12} & 0 & 0 & \dots & 0 & R_{11} \\ P_{21} & P_{22} & 0 & 0 & \dots & 0 & R_{21} \\ Q_{11} & Q_{12} & 0 & 0 & \dots & 0 & S \\ \tilde{H}_{11} & \tilde{H}_{12} & \tilde{H}_{13} & 0 & \dots & 0 & 0 \\ 0 & 0 & 0 & 1 & & 0 & 0 \\ \vdots & \vdots & \vdots & & \ddots & & \vdots \\ 0 & 0 & 0 & 0 & & 1 & 0 \end{pmatrix}, \tag{49}$$

where P_{ij}, R_{ij}, Q_{ij}, $\tilde{H}_{ij}$ $(i, j = 1, 2)$ denote the corresponding elements of matrices $\mathbf{P}$, $\mathbf{R}$, $\mathbf{Q}$ and $\tilde{\mathbf{H}} = \tilde{\mathbf{K}}\tilde{\mathbf{C}}$. Actually, $\tilde{H}_{11} = k_\mathrm{p}(1 + \delta_\mathrm{p})$, $\tilde{H}_{12} = k_\mathrm{d}(1 + \delta_\mathrm{v})$ and $\tilde{H}_{13} = k_\mathrm{a}(1+\delta_\mathrm{a})$. Stability of the system is determined by the eigenvalues of matrix $\mathbf{\Phi}$. The stability diagram with the stability boundaries for different sensory uncertainty radii is shown in Fig. 3. For the given parameters, no stable points were found for the uncertainty radii $\varepsilon = 0.25$. This means that a stick of length 1 m cannot be balanced by a PDA controller with $\Delta t = 10$ ms, $r = 10$, $k_\mathrm{a} = 0.75$ if the uncertainty in the perception of the angular position, angular velocity and angular acceleration is larger than 25 %. Note that the stable parameters show up in the domain $K_\mathrm{p} > mg$ and $K_\mathrm{d} > mg\tau$ (Sieber and Krauskopf 2005; Insperger et al. 2013).

4.3 Model predictive (MP) control

The MP controller is based on a prediction of state variables using an internal model of the system. It is known that optimum prediction for a system with input delay is obtained by solving the system equations over the delay period (Kleinman 1969; Manitius and Olbrot 1979). Consider first the continuous-time case. Assume that the system is given by Eq. (3) such that at time t, the most recent available output is $\mathbf{y}(t-\tau) = \mathbf{x}(t-\tau)$. In this case, the actual state $\mathbf{x}(t)$ can be predicted using $\mathbf{x}(t-\tau)$ as initial state and the control command $u(s)$, $s \in [t-\tau, t]$ in the form

$$\mathbf{x}_\mathrm{p}(t) = \mathrm{e}^{\tilde{\mathbf{A}}\tilde{\tau}}\mathbf{x}(t-\tau) + \int_{-\tilde{\tau}}^{0} \mathrm{e}^{-\tilde{\mathbf{A}}s}\tilde{\mathbf{B}}u(s+t)\mathrm{d}s, \tag{50}$$

where $\tilde{\mathbf{A}}$, $\tilde{\mathbf{B}}$ and $\tilde{\tau}$ are the estimated system and input matrices, and the estimated reflex delay used by the internal model and $\mathbf{x}_\mathrm{p}$ is the predicted state. Here, we consider a PD feedback of the predicted state. The corresponding MP controller reads

$$u(t) = \mathbf{K}\mathbf{x}_\mathrm{p}(t) = \mathbf{K}\mathrm{e}^{\tilde{\mathbf{A}}\tilde{\tau}}\mathbf{x}(t-\tau) + \mathbf{K}\int_{-\tilde{\tau}}^{0} \mathrm{e}^{-\tilde{\mathbf{A}}s}\tilde{\mathbf{B}}u(t+s)\mathrm{d}s, \tag{51}$$

where matrix $\mathbf{K}$ is given by Eq. (22). Note that the components k_p and k_d of $\mathbf{K}$ are now the proportional and the derivative gains for the predicted angular position and for the predicted angular velocity. The scheme of the prediction process for the MP controller is shown in Fig. 4. Note that this control concept requires the knowledge of the input u over the interval $[t-\tau, t]$. In the human neural system, this is provided by the efferent copies of the actual control commands.

If the parameters of the internal model match the actual system parameters, i.e., if $\tilde{\mathbf{A}} = \mathbf{A}$, $\tilde{\mathbf{B}} = \mathbf{B}$ and $\tilde{\tau} = \tau$, then the prediction gives the exact state, i.e., $\mathbf{x}_\mathrm{p}(t) = \mathbf{x}(t)$. In this case, the feedback of the predicted state eliminates the delay from the control loop and one ends up with the equation

$$\dot{\mathbf{x}}(t) = \mathbf{A}\mathbf{x}(t) + \mathbf{B}\mathbf{K}\mathbf{x}(t), \tag{52}$$

for which the characteristic roots can arbitrarily be assigned to any point within the complex plane by tuning the control

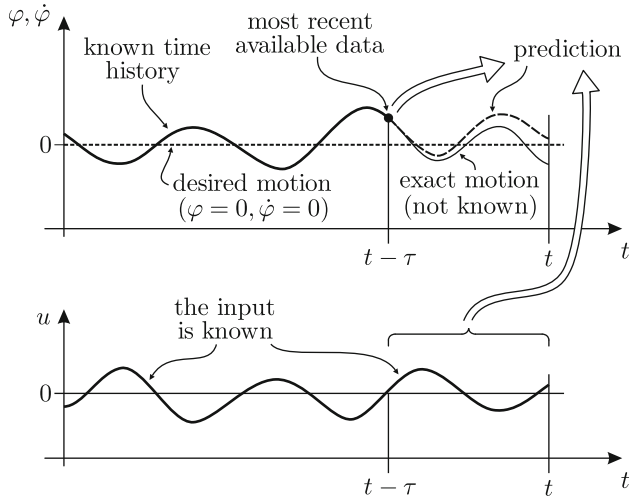

Fig. 4 Scheme of the prediction process for the MP controller

gains k_p and k_d in matrix $\mathbf{K}$. However, if the internal model is not perfectly accurate (i.e., $\tilde{\mathbf{A}} \neq \mathbf{A}$, $\tilde{\mathbf{B}} \neq \mathbf{B}$ or $\tilde{\tau} \neq \tau$), then Eqs. (3) and (51) define a system of RFDEs and the spectrum of the system become infinite.

We consider the case when the output is sampled at time instants $t_i = i\Delta t$, $i = 1, 2, \ldots$ and the input is piecewise constant, i.e., $u(t) = u(t_i)$, $t \in [t_i, t_{i+1})$. Similar to the PD and the PDA controllers, we assume that the angular position and the angular velocity are affected by sensory uncertainties described by Eqs. (21) and (20). Furthermore, we assume that the perceived efferent copies of the control command are

$$u_\mathrm{s}(t_i) = (1 + \delta_\mathrm{u})u(t_i), \tag{53}$$

where $|\delta_\mathrm{u}| \leq \varepsilon_\mathrm{u}$ with ε_u being the sensory uncertainty radii for the efferent copies. In this case, the state $\mathbf{x}(t_i)$ can be predicted by the internal model using the sampled output $\mathbf{y}(t_{i-r})$ as initial state and the perceived control commands $u_\mathrm{s}(t_{i-j})$, $j = 1, 2, \ldots, \tilde{r}$ as

$$\mathbf{x}_\mathrm{p}(t_i) = \tilde{\mathbf{P}}^{\tilde{r}}\mathbf{y}(t_{i-r}) + \sum_{j=1}^{\tilde{r}} \tilde{\mathbf{P}}^{j-1}\tilde{\mathbf{R}}u_\mathrm{s}(t_{i-j}), \tag{54}$$

where

$$\tilde{\mathbf{P}} = \mathrm{e}^{\tilde{\mathbf{A}}\Delta t}, \quad \tilde{\mathbf{R}} = \int_0^{\Delta t} \mathrm{e}^{\tilde{\mathbf{A}}(\Delta t - s)}\mathrm{d}s\, \tilde{\mathbf{B}}, \tag{55}$$

and $\tilde{r} = \mathrm{round}(\tilde{\tau}/\Delta t)$ is the discrete delay in the internal model. The corresponding control law reads

$$u(t_i) = \mathbf{K}\mathbf{x}_\mathrm{p}(t_i) = \mathbf{K}\tilde{\mathbf{P}}^{\tilde{r}}\mathbf{y}(t_{i-r}) + \mathbf{K}\sum_{j=1}^{\tilde{r}} \tilde{\mathbf{P}}^{j-1}\tilde{\mathbf{R}}u_\mathrm{s}(t_{i-j}). \tag{56}$$

If there are no sensory uncertainties (i.e., if $\mathbf{y}(t_{i-r}) = \mathbf{x}(t_{i-r})$ and $u_\mathrm{s}(t_{i-j}) = u(t_{i-j})$ with $j = 1, 2, \ldots, \tilde{r}$), then the actual control force for the stick balancing problem can be given by the expansion of formula (56) as

$$\begin{aligned} Q_x^\mathrm{fb}(t) = K_\mathrm{p}\Bigg(&\mathrm{ch}_{\tilde{r}}\varphi(t_{i-r}) + \frac{1}{\tilde{\alpha}}\mathrm{sh}_{\tilde{r}}\dot{\varphi}(t_{i-r}) \\ &+ \sum_{j=1}^{\tilde{r}} \frac{1}{\tilde{\alpha}^2}\left(\mathrm{ch}_j - \mathrm{ch}_{j-1}\right) Q_x^\mathrm{fb}(t_{i-j})\Bigg) \\ &+ K_\mathrm{d}\Bigg(\tilde{\alpha}\mathrm{sh}_{\tilde{r}}\varphi(t_{i-r}) + \mathrm{ch}_{\tilde{r}}\dot{\varphi}(t_{i-r}) \\ &+ \sum_{j=1}^{\tilde{r}} \frac{1}{\tilde{\alpha}}(\mathrm{sh}_j - \mathrm{sh}_{j-1})Q_x^\mathrm{fb}(t_{i-j})\Bigg), \quad t \in [t_i, t_{i+1}), \end{aligned} \tag{57}$$

where $K_\mathrm{p} = m\ell k_\mathrm{p}/6$ and $K_\mathrm{d} = m\ell k_\mathrm{d}/6$ are the actual control gains, $\tilde{\alpha} = \sqrt{\tilde{a}}$ with $\tilde{a}$ being the estimated system parameter used by the internal model and $\mathrm{ch}_j = \cosh(\tilde{\alpha} j\Delta t)$ and $\mathrm{sh}_j = \sinh(\tilde{\alpha} j\Delta t)$. This control law can be written in the form of the tapped delay-line controller (Mehta and Schaal 2002)

$$\begin{aligned} Q_x^\mathrm{fb}(t) = &\hat{K}_\mathrm{p}\varphi(t_{i-r}) + \hat{K}_\mathrm{d}\dot{\varphi}(t_{i-r}) \\ &+ \sum_{j=1}^{\tilde{r}} \hat{K}_{\mathrm{u},j} Q_x^\mathrm{fb}(t_{i-j}), \quad t \in [t_i, t_{i+1}), \end{aligned} \tag{58}$$

where

$$\hat{K}_\mathrm{p} = K_\mathrm{p}\mathrm{ch}_{\tilde{r}} + \tilde{\alpha}K_\mathrm{d}\mathrm{sh}_{\tilde{r}}, \tag{59}$$

$$\hat{K}_\mathrm{d} = \frac{1}{\tilde{\alpha}}K_\mathrm{p}\mathrm{sh}_{\tilde{r}} + K_\mathrm{d}\tilde{\alpha}\mathrm{ch}_{\tilde{r}} \tag{60}$$

are the proportional and the derivative control gains for the delayed state variables $\varphi(t_{i-r})$ and $\dot{\varphi}(t_{i-r})$ and

$$\hat{K}_{\mathrm{u},j} = K_\mathrm{p}\frac{1}{\tilde{\alpha}^2}\left(\mathrm{ch}_j - \mathrm{ch}_{j-1}\right) + K_\mathrm{d}\frac{1}{\tilde{\alpha}}\left(\mathrm{sh}_j - \mathrm{sh}_{j-1}\right) \tag{61}$$

are the control gains for the efferent copies of the control commands $u(t_{i-j})$, $j = 1, 2, \ldots, \tilde{r}$. In this sense, the MP controller is a special case of the tapped delay-line controller with the special control gains given by Eqs. (59), (60) and (61).

If $\tilde{\mathbf{A}} = \mathbf{A}$, $\tilde{\mathbf{B}} = \mathbf{B}$, $\tilde{\tau} = \tau$ and there are no sensory uncertainties in $\mathbf{x}_i$ and u_i, then Eq. (54) gives the exact state at $t = t_i$. In this case, the control law $u(t_i) = \mathbf{K}\mathbf{x}_\mathrm{p}(t_i)$ combined with Eq. (3) gives the discrete map $\mathbf{x}(t_{i+1}) = (\mathbf{P}+\mathbf{R}\mathbf{K})\mathbf{x}(t_i)$, which corresponds to a sampled output system (with a zero-order hold) without any feedback delay.

As it was explained in the Introduction, we assume that the internal model is accurate as a result of a long enough learning process (i.e., $\tilde{\mathbf{A}} = \mathbf{A}$, $\tilde{\mathbf{B}} = \mathbf{B}$, $\tilde{\tau} = \tau$, $\tilde{\mathbf{P}} = \mathbf{P}$ and $\tilde{\mathbf{R}} = \mathbf{R}$), and the uncertainties appear only in the sensory

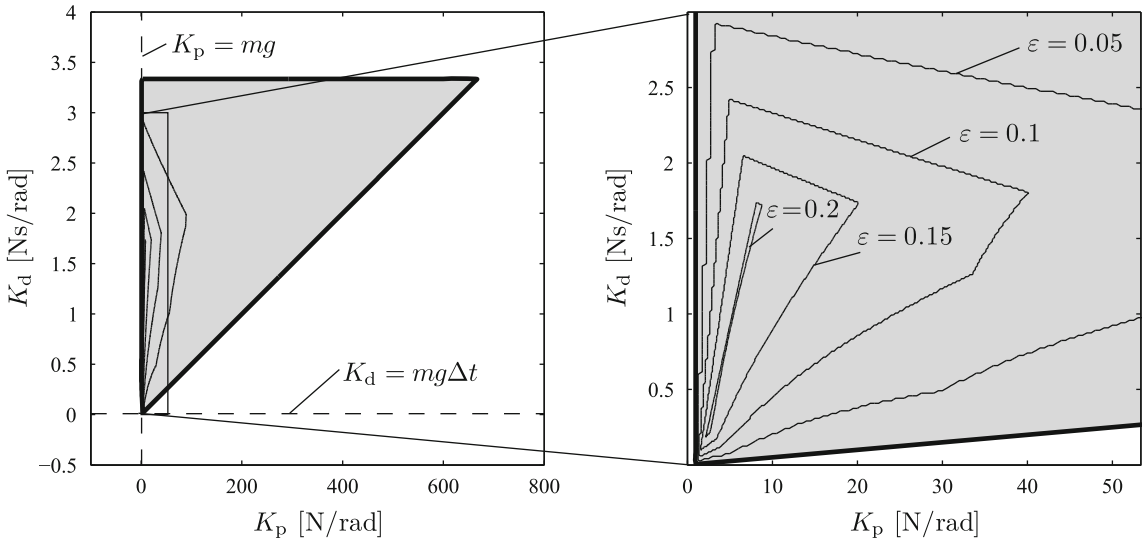

Fig. 5 Stability diagrams for the MP controller with $\Delta t = 10$ ms, $r = 10$, $\ell = 1$ m, $m = 0.1$ kg. The stable domain for zero uncertainty is indicated by *gray shading*, while the stability boundaries associated with different uncertainty radii $\varepsilon = \varepsilon_p = \varepsilon_v = \varepsilon_u$ are denoted by *thin lines*

inputs. In this case, the system described by Eqs. (3), (56), (21) and (53) can be rewritten as

$$\dot{\mathbf{x}}(t) = \mathbf{A}\mathbf{x}(t) + \mathbf{B}v(t_{i-r}), \quad t \in [t_i, t_{i+1}), \tag{62}$$

$$v(t_i) = \mathbf{K}\mathbf{P}^r\mathbf{C}\mathbf{x}(t_i) + \mathbf{K}\sum_{j=1}^{r}\mathbf{P}^{j-1}\mathbf{R}(1+\delta_u)v(t_{i-j}). \tag{63}$$

with $v(t_{i-r}) = u(t_i)$. The solution of this system over the sampling period $[t_i, t_{i+1})$ gives

$$\mathbf{x}(t_{i+1}) = \mathbf{P}\mathbf{x}(t_i) + \mathbf{R}v(t_{i-r}), \tag{64}$$

where $\mathbf{P}$ and $\mathbf{R}$ are defined in Eq. (33). Equations (64) and (63) define the $(r+2)$-dimensional discrete map

$$\mathbf{z}_{i+1} = \mathbf{\Phi}\mathbf{z}_i \tag{65}$$

with

$$\mathbf{z}_i = \begin{pmatrix} \varphi(t_i) \\ \dot{\varphi}(t_i) \\ v(t_{i-1}) \\ v(t_{i-2}) \\ \vdots \\ v(t_{i-r}) \end{pmatrix}, \quad \mathbf{\Phi} = \begin{pmatrix} P_{11} & P_{12} & 0 & 0 & \dots & 0 & R_{11} \\ P_{21} & P_{22} & 0 & 0 & \dots & 0 & R_{21} \\ T_{11} & T_{12} & V_1 & V_2 & \dots & V_{r-1} & V_r \\ 0 & 0 & 0 & 1 & & 0 & 0 \\ \vdots & \vdots & \vdots & & \ddots & & \vdots \\ 0 & 0 & 0 & 0 & & 1 & 0 \end{pmatrix}, \tag{66}$$

where P_{ij}, R_{ij}, T_{ij} $(i, j = 1, 2)$ denote the corresponding elements of matrices $\mathbf{P}$, $\mathbf{R}$ and $\mathbf{T} = \mathbf{K}\mathbf{P}^r\mathbf{C}$ and $V_j = \mathbf{K}\mathbf{P}^{j-1}\mathbf{R}(1+\delta_u)$. The stability of the system is determined by the eigenvalues of matrix $\mathbf{\Phi}$.

Figure 5 shows a sample stability diagram with the stability boundaries for different sensory uncertainty radii. For the given stick length, no stable points were found for the uncertainty radii $\varepsilon = 0.25$. This means that a stick of length 1 m cannot be balanced by a MP controller with $\Delta t = 10$ ms, $r = 10$ if the uncertainty in the perception of the angular position, angular velocity and efferent copies is larger than 25 %. Note that the stable parameters show up in the domain $K_p > mg$ and $K_d > mg\Delta t$.

4.4 Act-and-wait (AAW) control

The AAW controller is a special case of the time-varying controllers in which the feedback term is periodically switched on and off. The continuous-time AAW controller associated with Eq. (3) reads

$$u(t) = g(t)\mathbf{K}\mathbf{x}(t-\tau), \tag{67}$$

where $\mathbf{K}$ is given in Eq. (22), and

$$g(t) = \begin{cases} 0 & \text{if } 0 \le (t \mod T) < t_w, \\ 1 & \text{if } t_w \le (t \mod T) < t_w + t_a = T, \end{cases} \tag{68}$$

is the T-periodic act-and-wait switching function. Here, t_a and t_w are the lengths of the acting and the waiting periods, respectively, and $t_a + t_w = T$ is the length of one act-and-wait period. The main feature of the AAW controller is that the control is switched off for the waiting period, and a delayed PD controller is only working over the acting period. Equations (3) and (67) define the time-periodic RFDE

$$\dot{\mathbf{x}}(t) = \mathbf{A}\mathbf{x}(t) + g(t)\mathbf{B}\mathbf{K}\mathbf{x}(t-\tau). \tag{69}$$

As it was shown by Insperger (2006), if the waiting period is larger than the feedback delay, then the system can be described by a finite-dimensional discrete map. For instance, if $t_w \geq \tau$ and $t_a < \tau$, then the solution over one act-and-wait period can be given as $\mathbf{x}(T) = \mathbf{\Psi}(T)\mathbf{x}(0)$, where

$$\mathbf{\Psi}(T) = \mathrm{e}^{\mathbf{A}\mathbf{T}} + \int_{t_w}^{T} \mathrm{e}^{\mathbf{A}(T-s)}\mathbf{B}\mathbf{K}\mathrm{e}^{\mathbf{A}(s-\tau)}\,\mathrm{d}s \tag{70}$$

is the 2×2 monodromy matrix of the system. Stabilization of the system requires the placement of the 2 eigenvalues of matrix $\mathbf{\Psi}(T)$ within the unit circle of the complex plane by tuning the control gains k_p and k_d in $\mathbf{K}$. Thus, the infinite-dimensional control system is reduced to a two-dimensional system by introducing waiting periods into the feedback loop.

When sensory uncertainties are present, the control force with sampled output becomes

$$Q_x^{\mathrm{fb}}(t) = g(t)\left(K_p\varphi_s(t_{i-r}) + K_d\dot{\varphi}_s(t_{i-r})\right), \quad t \in [t_i, t_{i+1}), \tag{71}$$

where K_p and K_d are the proportional and the derivative control gains, respectively, and $\varphi_s(t)$ and $\dot{\varphi}_s(t)$ are the perceived angular position and the perceived angular velocity. The switching function $g(t)$ is given by Eq. (68). The waiting and the acting periods are chosen as $t_w = \tau = r\Delta t$ and $t_a = \Delta t$, respectively, which give the act-and-wait period $T = (r+1)\Delta t$. This corresponds to an intermittent control concept in the sense that control actions are taken only over the acting periods of length Δt, while the system is left open-loop over the waiting periods of length $r\Delta t$. The corresponding control law can be given as

$$u(t) = g(t)\mathbf{K}\mathbf{y}(t_{i-r}), \quad t \in [t_i, t_{i+1}), \tag{72}$$

where $\mathbf{K}$ is given in Eq. (22).

Due to the periodic switching of the control term, the solution of the system defined by Eqs. (3), (21) and (72) can be given in closed form. In the first act-and-wait period, the system is governed by

$$\dot{\mathbf{x}}(t) = \mathbf{A}\mathbf{x}(t), \qquad t \in [0, t_r), \tag{73}$$

$$\dot{\mathbf{x}}(t) = \mathbf{A}\mathbf{x}(t) + \mathbf{B}\mathbf{K}\mathbf{C}\mathbf{x}(0), \qquad t \in [t_r, t_{r+1}). \tag{74}$$

The solution at $t = T = t_{r+1}$ can be written as

$$\mathbf{x}(T) = \mathbf{\Phi}\mathbf{x}(0), \tag{75}$$

where $\mathbf{\Phi} = \mathbf{P}^{r+1} + \mathbf{R}\mathbf{K}\mathbf{C}$ with $\mathbf{P}$ and $\mathbf{R}$ given in Eq. (33). The matrix $\mathbf{\Phi}$ is actually a 2×2 monodromy matrix of the system. Hence, the system is stable if the eigenvalues of $\mathbf{\Phi}$ are in modulus less than 1.

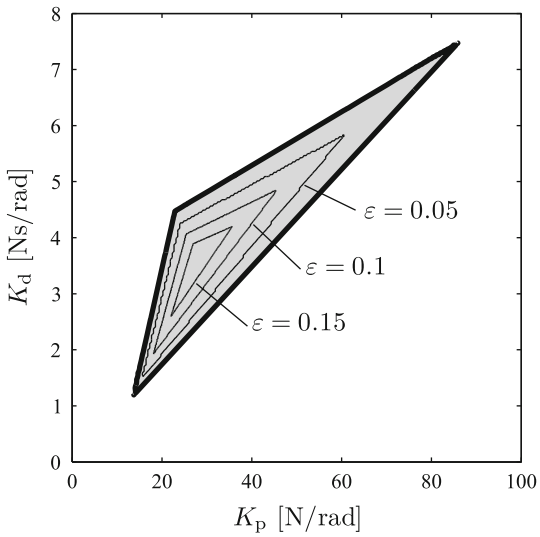

Fig. 6 Stability diagrams for the AAW controller with $\Delta t = 10$ ms, $r = 10$, $\ell = 1$ m, $m = 0.1$ kg, $t_a = 10$ ms, $t_w = 100$ ms. The stable domain for zero uncertainty is indicated by *gray shading*, while the stability boundaries associated with different uncertainty radii $\varepsilon = \varepsilon_p = \varepsilon_v$ are denoted by *thin lines*

Figure 6 shows the stability diagram with the stability boundaries for different sensory uncertainty radii. For the given stick length, no stable points were found for the uncertainty radii $\varepsilon = 0.2$. This means that a stick of length 1 m cannot be balanced by the AAW controller with $\Delta t = 10$ ms, $r = 10$, $t_w = r\Delta t$ and $t_a = \Delta t$ if the uncertainty in the perception of the angular position and the angular velocity is larger than 20 %. Note that the proportional and differential gains for the stable domains are essentially larger than that of the PD or the PDA controllers. This is due to the fact that actions are performed only for a period of length $t_a = 10$ ms, while no control action is performed for a period of length $t_w = 100$ ms.

4.5 Intermittent predictive controller

Intermittent predictive controller makes use of sampled feedback of the state variables, but uses a special system-matched hold rather than zero-order hold (Gawthrop and Wang 2007; Gawthrop et al. 2011). If the system is described by Eq. (3), then the intermittent control input is formulated as

$$u(t) = \mathbf{K}\mathrm{e}^{(\tilde{\mathbf{A}}+\tilde{\mathbf{B}}\mathbf{K})(t-t_i)}\mathbf{x}_{\mathrm{ip}}(t_i), \quad t \in [t_i, t_{i+1}), \tag{76}$$

where $\tilde{\mathbf{A}}$ and $\tilde{\mathbf{B}}$ are the estimated system and input matrices used by the internal model, and $\mathbf{x}_{\mathrm{ip}}(t_i)$ is the intermittent prediction of the state at time instant t_i based on the delayed output $\mathbf{y}(t_i - \tau)$. Here, similar to the previous cases, we assume that the length of the open-loop interval is $\Delta t = \tau/r$. Thus, the prediction is updated at each sampling instant $t_i = i\Delta t$

based on the most recent available output $\mathbf{y}(t_{i-r})$. This is in contrast with the concept by Gawthrop et al. (2011), where the sampling period is chosen as $\Delta t \geq \tau$ in order to obtain a relatively simple intermittent prediction.

The delay used for the prediction by the internal model is denoted by $\tilde{\tau}$, and the corresponding discrete delay is $\tilde{r} = \text{round}(\tilde{\tau}/\Delta t)$. The prediction is performed over a delay period based on the system-matched hold assumption by solving the system

$$\dot{\mathbf{x}}_{\text{ip}}(t) = \tilde{\mathbf{A}}\mathbf{x}_{\text{ip}}(t) + \tilde{\mathbf{B}}\mathbf{K}\mathrm{e}^{(\tilde{\mathbf{A}}+\tilde{\mathbf{B}}\mathbf{K})(t-t_i-\tau)}\mathbf{y}(t_{i-r}), \quad t \in [t_{i-\tilde{r}}, t_i), \tag{77}$$

for the initial state $\mathbf{x}_{\text{ip}}(t_{i-r}) = \mathbf{y}(t_{i-r})$. The predicted state can be given as

$$\mathbf{x}_{\text{ip}}(t_i) = \mathrm{e}^{\tilde{\mathbf{A}}\tilde{r}\Delta t}\left(\mathbf{I} + \int_0^{\tilde{r}\Delta t} \mathrm{e}^{-\tilde{\mathbf{A}}s}\tilde{\mathbf{B}}\mathbf{K}\mathrm{e}^{(\tilde{\mathbf{A}}+\tilde{\mathbf{B}}\mathbf{K})s}\mathrm{d}s\right)\mathbf{y}(t_{i-r}), \tag{78}$$

where $\mathbf{I}$ denotes the identity matrix. This type of prediction is also called simplified or intermittent predictor, since the convolution integral in the second term can be computed by a matrix exponential. Actually, due to the intermittency of the controller, the predicted state can also be given as

$$\mathbf{x}_{\text{ip}}(t_i) = \left(\mathbf{E}_{\text{pp}} + \mathbf{E}_{\text{ph}}\right)\mathbf{y}(t_{i-r}), \tag{79}$$

where $\mathbf{E}_{\text{pp}}$ and $\mathbf{E}_{\text{ph}}$ are the partitions of the matrix

$$\mathbf{E} = \mathrm{e}^{\mathbf{A}_{\text{ph}}\tilde{r}\Delta t} = \begin{pmatrix}\mathbf{E}_{\text{pp}} & \mathbf{E}_{\text{ph}} \\ \mathbf{E}_{\text{hp}} & \mathbf{E}_{\text{hh}}\end{pmatrix}, \tag{80}$$

with

$$\mathbf{A}_{\text{ph}} = \begin{pmatrix}\tilde{\mathbf{A}} & \tilde{\mathbf{B}}\mathbf{K} \\ \mathbf{0} & \tilde{\mathbf{A}} + \tilde{\mathbf{B}}\mathbf{K}\end{pmatrix}. \tag{81}$$

Using Eqs. (76), (79) and the definition of $u(t)$ in Eq. (2), the actual control force can be given as

$$Q_x^{\text{fb}}(t) = \frac{m\ell}{6}\mathbf{K}\mathrm{e}^{(\tilde{\mathbf{A}}+\tilde{\mathbf{B}}\mathbf{K})(t-t_i)}\left(\mathbf{E}_{\text{pp}} + \mathbf{E}_{\text{ph}}\right)\mathbf{y}(t_{i-r}), \quad t \in [t_i, t_{i+1}). \tag{82}$$

The solution of Eq. (3) with the control law (76) over the sampling period $[t_i, t_{i+1})$ can be given as

$$\mathbf{x}(t_{i+1}) = \mathrm{e}^{\mathbf{A}\Delta t}\mathbf{x}(t_i) + \left(\int_0^{\Delta t} \mathrm{e}^{\mathbf{A}(\Delta t-s)}\mathbf{B}\mathbf{K}\mathrm{e}^{(\tilde{\mathbf{A}}+\tilde{\mathbf{B}}\mathbf{K})s}\mathrm{d}s\right)\mathbf{x}_{\text{ip}}(t_i). \tag{83}$$

Similar to the simplified prediction, the convolution integral can be given in an explicit way as

$$\mathbf{x}(t_{i+1}) = \mathbf{F}_{\text{ss}}\mathbf{x}(t_i) + \mathbf{F}_{\text{sh}}\mathbf{x}_{\text{ip}}(t_i), \tag{84}$$

where $\mathbf{F}_{\text{ss}}$ and $\mathbf{F}_{\text{sh}}$ are the partitions of the matrix

$$\mathbf{F} = \mathrm{e}^{\mathbf{A}_{\text{sh}}\Delta t} = \begin{pmatrix}\mathbf{F}_{\text{ss}} & \mathbf{F}_{\text{sh}} \\ \mathbf{F}_{\text{hs}} & \mathbf{F}_{\text{hh}}\end{pmatrix}, \tag{85}$$

with

$$\mathbf{A}_{\text{sh}} = \begin{pmatrix}\mathbf{A} & \mathbf{B}\mathbf{K} \\ \mathbf{0} & \tilde{\mathbf{A}} + \tilde{\mathbf{B}}\mathbf{K}\end{pmatrix}. \tag{86}$$

Equations (84), (79) and (21) define the $(2 + 2r)$-dimensional discrete map

$$\mathbf{z}_{i+1} = \boldsymbol{\Phi}\,\mathbf{z}_i \tag{87}$$

with

$$\mathbf{z}_i = \begin{pmatrix}\mathbf{x}(t_i) \\ \mathbf{x}(t_{i-1}) \\ \mathbf{x}(t_{i-2}) \\ \vdots \\ \mathbf{x}(t_{i-r})\end{pmatrix}, \quad \boldsymbol{\Phi} = \begin{pmatrix}\mathbf{F}_{\text{ss}} & \mathbf{0} & \mathbf{0} & \dots & \mathbf{0} & \mathbf{W} \\ \mathbf{I} & \mathbf{0} & \mathbf{0} & \dots & \mathbf{0} & \mathbf{0} \\ \mathbf{0} & \mathbf{I} & \mathbf{0} & \dots & \mathbf{0} & \mathbf{0} \\ \vdots & & & \ddots & \vdots & \vdots \\ \mathbf{0} & \mathbf{0} & \mathbf{0} & \dots & \mathbf{I} & \mathbf{0}\end{pmatrix}, \tag{88}$$

where $\mathbf{W} = \mathbf{F}_{\text{sh}}\left(\mathbf{E}_{\text{pp}} + \mathbf{E}_{\text{ph}}\right)\mathbf{C}$. Note that $\mathbf{F}_{\text{ss}} = \mathbf{P}$ defined in Eq. (33). The stability of the system is determined by the eigenvalues of matrix $\boldsymbol{\Phi}$.

Note that the IP and the AAW controllers are similar in the sense that both controllers have a generalized hold interpretation (Gawthrop 2010). However, in contrast with the IP controller, the AAW controller relies on a feedback of the delayed state and does not use an internal model for the prediction of the actual state.

As mentioned, if $\Delta t \geq \tau$, then the intermittent prediction has a simple form Gawthrop et al. (2011). For instance, if $\Delta t = \tau$, then matrix $\boldsymbol{\Phi}$ becomes a 4×4 matrix. In this case, however, the output is sampled at every $\Delta t = \tau = 100$ ms only. In our model, we assume that the output is sampled at every $\Delta t = \tau/r = 10$ ms; thus, the intermittent predictor uses more recent output data, which improves stability properties but, at the same time, the size of the monodromy matrix describing the system dynamics is larger.

For the stability calculation, we assume that the internal model is accurate as a result of a long enough learning process as explained in the Introduction (i.e., $\tilde{\mathbf{A}} = \mathbf{A}$, $\tilde{\mathbf{B}} = \mathbf{B}$ and $\tilde{\tau} = \tau$), and the uncertainties appear only in the sensory inputs described by the output matrix $\mathbf{C}$. Figure 7 shows a sample stability diagram with the stability boundaries for different sensory uncertainty radii. For the given stick length,

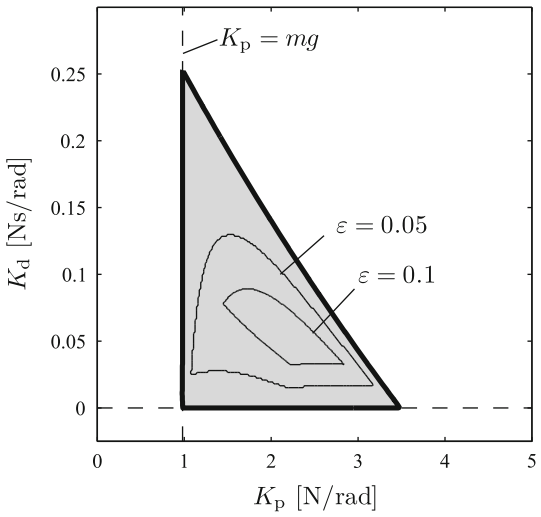

Fig. 7 Stability diagrams for the IP controller with $\Delta t = 10$ ms, $r = 10$, $\ell = 1$ m, $m = 0.1$ kg. The stable domain for zero uncertainty is indicated by *gray shading*, while the stability boundaries associated with different uncertainty radii $\varepsilon = \varepsilon_p = \varepsilon_v$ are denoted by *thin lines*

no stable points were found for the uncertainty radii $\varepsilon = 0.15$. This means that a stick of length 1 m cannot be balanced by the IP controller with $\Delta t = 10$ ms, $r = 10$ if the uncertainty in the perception of the angular position and angular velocity is larger than 15 %. Note that the stable parameters show up in the domain $K_p > mg$ and $K_d > 0$.

5 Critical length

The critical stick length, ℓ_{crit}, is the shortest stick length that can be stabilized by a control mechanism for a given τ. We used the following procedure to estimate ℓ_{crit} for the PD, PDA, MP, AAW and IP controllers as a function of τ for different sensory uncertainty radii (ε). We assumed that the uncertainty radius for each of the different sensory inputs is the same, namely $\varepsilon_p = \varepsilon_v = \varepsilon_a = \varepsilon_u = \varepsilon$.

1. The uncertainty radius ε was fixed.
2. The length of the stick was fixed, and the stability diagram in the plane (K_p, K_d) was determined according to Sects. 4.1–4.5 for the case without sensory uncertainties (i.e., for $\delta_i = 0$, $i = $ p, v, a, u). The resolution step in the plane (K_p, K_d) was $\Delta K_p = mg/100$ and $\Delta K_d = mg\tau/100$. Considering the structure of the stability diagrams in Figs. 2, 3, 5, 6 and 7, this resolution is a reasonable choice. For the PDA controller, the acceleration control gain was set such that $k_a + \varepsilon_a \leq 0.95$ (note that $k_a + \varepsilon_a \geq 1$ results in an unstable control process in case of $\delta_a = \varepsilon_a$). For the different uncertainty radii $\varepsilon = 0.01, 0.02, 0.05, 0.1, 0.15, 0.2$ in Fig. 8, the acceleration gains were $k_a = 0.9, 0.9, 0.9, 0.85, 0.8, 0.75$, respectively. For the AAW controller, the lengths of the waiting and the acting periods were $t_w = \Delta t = 10$ ms and $t_a = r\Delta t = \tau$.
3. At the parameter points, where the system was found to be stable, stability was determined for all possible combinations of sensory uncertainties $\delta_i \in \{-\varepsilon_i, 0, \varepsilon_i\}$ ($i = $ p, v, a, u). For the PD, the AAW and the IP controllers, the combinations of $\delta_p \in \{-\varepsilon_p, 0, \varepsilon_p\}$ and $\delta_v \in \{-\varepsilon_v, 0, \varepsilon_v\}$ gave $3 \times 3 = 9$ different cases of sensory uncertainties. For the PDA and the MP controllers, $3 \times 3 \times 3 = 27$ different cases were analyzed, since in these cases, the uncertainties in the acceleration ($\delta_a \in \{-\varepsilon_a, 0, \varepsilon_a\}$) and in the efference copies ($\delta_u \in \{-\varepsilon_u, 0, \varepsilon_u\}$) were also considered, respectively.
4. If there was at least one point in the plane (K_p, K_d) where the system was stable for all the possible combinations of the sensory uncertainties, then the system was declared robustly stable for the given uncertainties. In this case, the length of the stick was reduced, and the steps 2 and 3 were repeated for the new stick length.
5. Steps 2, 3 and 4 were repeated until no more robustly stable point was found. The critical length is the one, for which there is a stable point in the plane (K_p, K_d), which remains stable for the given sensory uncertainties, but for a 1-cm shorter stick, there is no robustly stable point.

Figure 8 shows ℓ_{crit} for the different controllers as a function of τ and ε. For $\varepsilon \leq 0.2$, PD and IP provided the least robust control (longest ℓ_{crit}) for τ in the experimentally observed range (between the vertical dashed lines in Fig. 8). For $\varepsilon \leq 0.1$, the MP control had the shortest ℓ_{crit} for this range of τ. However, for $\varepsilon = 0.15$, PDA control was equally as good as MP control, and for $\varepsilon = 0.2$, PDA control was the more robust.

The ε-dependent differences in the behavior of the MP and PDA controllers suggests that there is a trade-off between the benefits of model predictive control on the one hand and the attendant amplification of the sensory input error on the other. For $\varepsilon \leq 0.15$, the benefits of model prediction outweigh the costs of sensory input error amplification, and hence, MP is the more robust controller. However, once the sensory input error becomes large enough, the sensory input error amplification dominates over the benefits of model predictive control. Consequently, in the context of high sensory input error, delayed state feedback control, such as PDA, becomes more effective.

6 Sampling period

All of the models, we have considered assume a single, fixed delay. However, in reality, the neural delay for stick balancing is likely to be more complicated: a distributed or even a

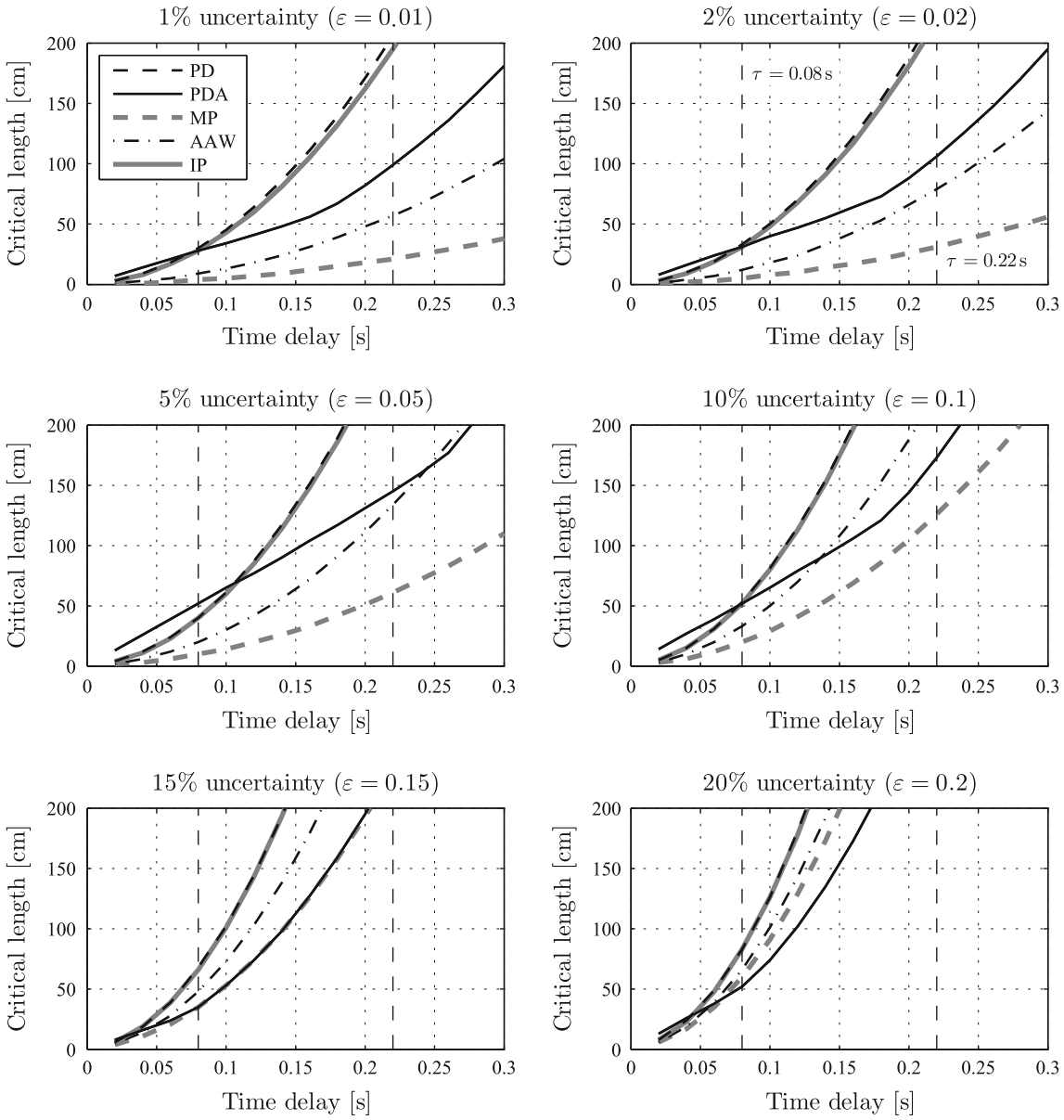

Fig. 8 Critical lengths as function of time delay for different sensory uncertainties (ε). The vertical *dashed line* indicates the range of τ measured for human stick balancing: $\tau \approx 0.08$–$0.1\,\mathrm{s}$ for balancing on a fingertip (Cabrera and Milton 2004), and $\tau \approx 0.22\,\mathrm{s}$ for balancing on the surface of a table tennis racket (Mehta and Schaal 2002)

state-dependent delay may be more appropriate. The introduction of Δt enables a discrete approximation to the continuous dynamics, which is not very sensitive to the nature of the time delays. In other words, this is a useful first step approximate to explore the effects of sensory uncertainty on balance control. This point having been made, it is clearly very important to determine to what extent the value of Δt affects the conclusions in Fig. 8.

Figure 9 shows a plot of ℓ_{crit} versus Δt for the five models of balance control determined for two different time delays when the sensory uncertainty is 10 %. The uncertainty for neurons in the central nervous systems is ≈7–13 % (Arieli et al. 1996; Otmakhov et al. 1993; Shadlen and Newsome 1998; Werner and Mountcastle 1963). This estimate is obtained from the coefficient of variation calculated for neural spike train and neural population responses to external stimuli. As can be seen, the effect of changing Δt over the range of 1–20 ms on ℓ_{crit} is very small.

7 Conclusions

The design of a feedback controller suitable for balancing a stick of a given length at the fingertip depends on the time

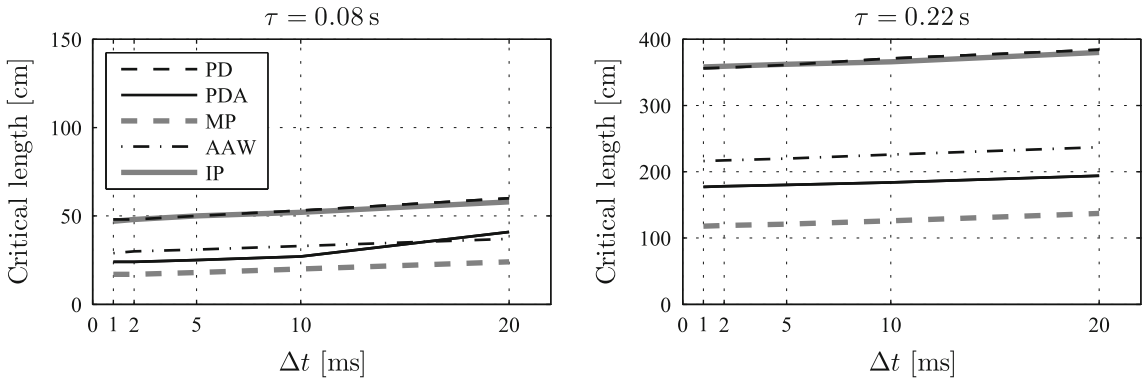

Fig. 9 Critical lengths as function of sampling period for 10 % sensory uncertainty ($\varepsilon = 0.1$). The acceleration gain for the PDA controller was $k_a = 0.75$

delay (τ) and the uncertainty in the sensory input (ε). Our observations suggest that MP control is the most robust for stick balancing at the fingertip when $\tau \approx 0.08$ s, namely the delay observed for human stick balancing at the fingertip. Although the sensitivity of MP controllers to sensory uncertainty has been used to motivate the need for noise reduction strategies (Bays and Wolpert 2007), such as those based on population density coding (Milton and Mackey 2000; Shadlen and Newsome 1998; Werner and Mountcastle 1963), the Kalman filter (Mehta and Schaal 2002) and Bayesian approaches (Krill and Peuget 2004), our observations suggest that these additional procedures are not necessary. Specifically, our observations indicate that tapped delay-line controllers are sufficient to stabilize stick of length 0.25–0.5 m, i.e., the shortest lengths that sticks can be balanced at the fingertip by skilled human stick balancers. The uncertainties takes the form of a multiplicative term in the system output. Although controllers robust to the effects of multiplicative uncertainties have been developed (Freudenberg and Looze 1988; Gawthrop et al. 2011; Goodwin et al. 2001; Skogestad and Postlewaite 1996; Stein 2003), it is not clear whether such robust controllers are appropriate for stick balancing (Cluff and Balasubramaniam 2010; Cabrera and Milton 2002, 2004).

The observation that only certain individuals following long periods of practice (weeks to months) can balance sticks of this length is consistent with the suggestion that critically important gains and other parameters in the controller are adjusted using a feedback error-learning schemes (Kawato 1990; Gomi and Kawato 1993; Valero-Cuevas et al. 2009). Note that here we considered only linear control models, but nonlinear controllers such as the ones proposed by Bottaro et al. (2008), Asai et al. (2009), Suzuki et al. (2012) are also promising alternatives for the human controller.

We emphasize that the above observations apply specifically to models for stick balancing expressed in terms of Eq. (2). In other words, it is not possible to interpret our observations as proof that the nervous system does indeed use MP-type feedback controllers. An important limitation of these models is that they do not correctly describe the nature of the interaction between the fingertip and stick, namely the nature of the pivot point for the inverted pendulum. For Eq. (2), the stick is physically attached in a frictionless manner to the pivot point, and hence, recovery is possible even from initial displacement angles, $\varphi(0)$, as large as 180°. In contrast, for human stick balancing the stick falls off the fingertip once, $\varphi(t)$ becomes sufficiently large: our experience suggests that expert stick balancers cannot tolerate $\varphi(0) \geq 20°$. Since the stick is not physically attached to the fingertip, it becomes necessary to consider contributions to control related to friction (Campbell et al. 2008; Landry et al. 2005). The addition of friction terms of the form $k\dot{\varphi}(t)$ to Eq. (2), where k is a small, positive friction constant, can have profound effects on stability. For example, the critical length is significantly smaller if k is large. The importance of the contact between stick and fingertip for stick balancing is readily demonstrated by the dramatic increase in difficulty encountered when balancing a stick on a smooth, polished surface, such as a plastic plate.

Mehta and Schaal (2002) were the first neuroscientists to propose that MP models are involved in the control of stick balancing by humans, but were unable to identify the precise nature of the controller. Their difficulties may have stemmed from the fact that they only considered a 1-m stick balanced on the surface of a table tennis racket. The advantage of the use of the table tennis racket is that it minimizes input from mechanoreceptors and hence $\tau \approx 0.22$ s. In our experience, the shortest stick that can be balanced by a highly skilled stick balancer on a table tennis racket is ≈0.1–0.2 m longer than the shortest stick that can be balanced at the fingertip. From Fig. 8, we see that this could be accomplished by a MP controller in combination with a noise reduction algorithm [e.g., a Kalman filter (Mehta and Schaal 2002)] so that $\varepsilon \leq 0.02$. However, it is unlikely that the nature of the contact between stick and fingertip is the same as that between stick and table tennis racket. In other words, the friction provided

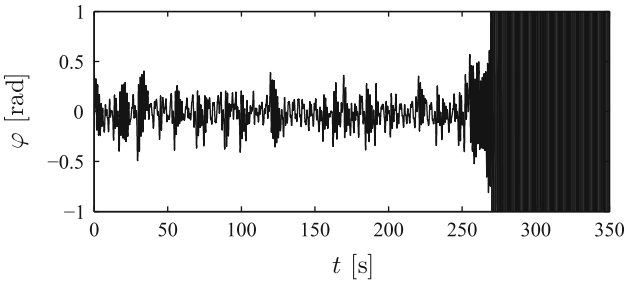

Fig. 10 Long-lived transient motion in case of a PDA control model with sensory dead zone $\varphi_{dz} = 0.01$ (rad), $\dot{\varphi}_{dz} = 0.01$ (rad/s), $\ddot{\varphi}_{dz} = 0.01$ (rad/s^2). The system without the dead zone is unstable; however, for the given dead zone, bounded transient motion survives for 250 s. Parameters: $\ell = 1$ m, $\tau = 0.22$ s, $k_p = 61$, $k_d = 14.9$, $k_a = 0.9$

by the rubberized surface of the table tennis racket may in large part explain the ability to balance short sticks in this scenario.

It is difficult to estimate the critical stick length, ℓ_{crit}, for human stick balancing experimentally. As an illustration consider the following. Our most-skilled stick balancer can balance 100 % of stick balancing trials longer than 240 s for a 0.4-m stick, 20 % of trials for a 0.315-m stick, and 0 % of trials for a 0.299-m stick. However, for a 0.299-m stick, this individual achieves a mean stick balancing time of 69 s, which is considerably longer than the time required for an uncontrolled stick to topple over (<2 s for sticks of length 0.2–1 m). The fundamental problem is to distinguish an asymptotically stable solution from a long-lived transient. Transient maintenance of the upright position lasting minutes readily arises in noisy, time-delayed dynamical systems (Cabrera and Milton 2002; Milton et al. 2008). Figure 10 shows that long-lived transient stabilizations of a stick under PDA control can occur in the presence of a sensory dead zone. In both of these situations, these transients arise in a dynamical system that is unstable in the noise-free case and without deadzone. Similar behavior is typical in robotic balancing, where the digital effects, i.e., the sampling, the processing delay and the round-off error result in a small amplitude chaotic motion around the equilibrium, which is called micro-chaos (Csernak and Stepan 2010).

As subjects become more skilled in the performance of a complex voluntary motor task, they become more goal-oriented and less dependent on intentionally directed corrective movements (Fitts and Posner 1967). This observation suggests that the control mechanisms themselves may change with practice as skill increases. For example, a subject may initially use a sensory feedback controller, such as PD or PDA, and then with learning develop an internal model which enables a switch to a MP controller. A practical problem has been the scarcity of methods to determine when such changes in control strategy occur (Cabrera and Milton 2004; Cluff and Balasubramaniam 2010). We suggest that if the time delay (τ), critical length (ℓ_{crit}) and sensory uncertainly level (ε) is known, then the possible feedback controller(s) that can meet these criteria can be determined. In particular, it is possible to determine at which skill level a state sensory feedback controller (PD, PDA) is no longer capable. All of these parameters can be measured in the laboratory: τ from corrections made in response to an external perturbation, ℓ_{crit} from the shortest time length that can be maintained for a specified time and the uncertainly from the variance of the fluctuations in the vertical displacement angle. Since skill levels remain fairly constant over testing periods administered on the same day, it becomes possible using τ, ℓ_{crit} and uncertainty estimates to follow the changes in feedback objectively as the subject becomes skilled. Thus, we anticipate that determining these parameters will provide insights into the development of skill with practice.

Acknowledgments The authors gratefully acknowledge support from the Hungarian National Science Foundation under grant OTKAK105433 (TI), the Hungarian-American Enterprise Scholarship Fund (HAESF) (TI), the William R Kenan, Jr Charitable Trust (JM), the National Science Foundation (JM, NSF-1028970) and the Invitation Award to Distinguished Scientists by the Hungarian Academy of Sciences (JM).

References

Abed EH, Wang H, Tesi A (2000) Control of bifurcations and chaos. In: Levine WS (ed) The control handbook. CRC and IEEE Press, Boca Raton, FL, pp 951–966

Arieli A, Sterkin A, Grinvald A, Aertsen A (1996) Dynamics of ongoing activity: explanation of the large variability in evoked cortical responses. Science 273:1868–1871

Arstein Z (1982) Linear systems with delayed controls: a reduction. IEEE T Autom Control 27:869–879

Asai Y, Tasaka Y, Nomura K, Nomura T, Casidio M, Morasso P (2009) A model of postural control in quiet standing: robust compensation of delay-induced instability using intermittent activation of feedback control. PLoS ONE 4:e6169

Bays PM, Wolpert DM (2007) Computational principles of sensorimotor control that minimize uncertainty and variability. J Physiol 578(2):387–396

Beilock S (2011) Choke: what the secrets of the brain reveal about getting it right when you have to. Free Press, Simon & Schuster, New York

Bottaro A, Yasutake Y, Nomura T, Casadio M, Morasso P (2008) Bounded stability of the quiet standing posture: an intermittent control model. Hum Mov Sci 27:473–495

Cabrera JL, Milton JG (2002) On-off intermittency in a human balancing task. Phys Rev Lett 89:158702

Cabrera JL, Milton JG (2004) Human stick balancing: tuning Lévy flights to improve balance control. CHAOS 14(3):691–698

Cabrera JL, Bormann R, Eurich C, Ohira T, Milton J (2004) State-dependent noise and human balance control. Fluct Noise Lett 4:L107–L117

Campbell SA, Crawfor S, Morris K (2008) Friction and the inverted pendulum stabilization problem. ASME J Dyn Syst Meas ContROL 130(054):501

Cluff T, Balasubramaniam R (2010) Motor learning characterized by changing Lévy distributions. PLoS ONE 4:e5998

Csernak G, Stepan G (2010) Digital control as source of chaotic behaviour. Int J Bifurcat Chaos 20:13651378
Engelborghs K, Dambrine M, Roose D (2001) Limitations of a class of stabilization methods for delay systems. IEEE Trans Autom Control 46:336–339
Enikov E, Stepan G (1998) Micro-chaotic motion of digitally controlled machines. J Vib Control 2:427–443
Fitts PM, Posner MI (1967) Human performance. Brooks/Cole, Belmont, CA
Freudenberg JS, Looze DP (1988) Frequency domain properties of scalar and multivariable feedback systems. Springer, Berlin
Gawthrop P (2010) Act-and-wait and intermittent control: some comments. IEEE Trans Control Syst Technol 18:1195–1198
Gawthrop P, Loram I, Lakie M, Gollee H (2011) Intermittent control: a computational theory of human control. Biol Cybern 104:31–51
Gawthrop PJ, Wang L (2007) Intermittent model predictive control. Proc Inst Mech Eng I J Syst Control Eng 221:1007–1018
Gomi H, Kawato M (1993) Neural network control for a closed-loop system using feedback-error-learning. Neural Netw 6:933–946
Goodwin GC, Graebe SF, Salgado ME (2001) Control system design. Prentice Hall, New Jersey
Hale JK, Lunel SMV (1993) Introduction to functional differential equations. Springer, New York
Hochberg LR, Bacher D, Jarosiewicz B, Masse NY, d Simeral J, Vogel J, Haddadin S, Liu J, Cash SS, van der Smagt P, Donoghue JP (2012) Reach and grasp by people with tetraplegia using a neurally controlled robotic arm. Nature 485:372–377
Insperger T (2006) Act and wait concept for time-continuous control systems with feedback delay. IEEE Trans Control Syst Technol 14:974–977
Insperger T (2011) Stick balancing with reflex delay in case of parametric forcing. Commun Nonlinear Sci 16:2160–2168
Insperger T, Stepan G (2007) Act-and-wait control concept for discrete-time systems with feedback delay. IET Control Theory A 1(3):553–557
Insperger T, Stepan G (2011) Semi-discretization for time-delay systems. Springer, New York
Insperger T, Milton J, Stepan G (2013) Acceleration feedback improves balancing against reflex delay. J R Soc Interface 10(79):20120763
Jordan MI (1996) Computational aspects of motor control and motor learning. In: Heuer H, Keele S (eds) Handbook of perception and action: motor skills. Academic Press, New York, pp 71–120
Kawato M (1990) Feedback-error-learning neural network for supervised learning. In: Eckmiller R (ed) Advanced neural computers. Elsevier, Amsterdam, pp 365–372
Kawato M (1999) Internal models for motor control and trajectory planning. Curr Opin Neurobiol 9(6):718–727
Kleinman DL (1969) Optimal control of linear systems with time-delay and observation noise. IEEE Trans Automat Contr 14:524–527
Krill DC, Peuget A (2004) The Bayesian brain: the role of uncertainty in neural coding and computation. Trends Neurosci 27: 712–719
Krstic M (2009) Delay compensation for nonlinear, adaptive, and PDE systems. Birkhäuser, Boston
Kuiken TA, Miller LA, Lipschutz RD, Lock BA, Stubblefield K, Marasso PD, Zhou P, Dumanian G (2007) Targeted reinnervation for enhanced prosthetic arm function in a woman with a proximal amputation: a case study. Lancet 369:371–380
Landry M, Campbell SA, Morris K, Aguilar CO (2005) Dynamics of an inverted pendulum with delayed feedback control. SIAM J Appl Dyn Syst 4:333–351
Manitius AZ, Olbrot AW (1979) Finite spectrum assignment problem for systems with delays. IEEE Trans Autom Control AC–24:541–553
McDonnell MD, Ward LM (2011) The benefits of noise in neural systems: bridging theory and experiment. Nat Rev Neurosci 12:415–426
Mehta B, Schaal S (2002) Forward models in visuomotor control. J Neurophysiol 88:942–953
Miall R, Weir DJ, Wolpert DM, Stein JF (1993) Is the cerebellum a Smith predictor? J Mot Behav 25(3):203–216
Miall RC, Jackson JK (2006) Adaptation to visual feedback delays in manual tracking: evidence against the Smith predictor model of human visually guided action. Exp Brain Res 172:77–84
Michiels W, Niculescu SI (2003) On the delay sensitivity of Smith predictors. Int J Syst Sci 34(8–9):543–551
Michiels W, Niculescu SI (2007) Stability and stabilization of time-delay systems: an eigenvalue-based approach. SIAM Publications, Philadelphia
Michiels W, Roose D (2003) An eigenvalue based approach to the robust stabilization of linear time-delay systems. Int J Control 76(7):678–686
Milton J, Solodkin A, Hlustik P, Small SL (2007) The mind of expert motor performance is cool and focused. NeuroImage 35:804–813
Milton J, Cabrera JL, Ohira T, Tajima S, Tonosaki Y, Eurich CW, Campbell SA (2009a) The time-delayed inverted pendulum: implications for human balance control. Chaos 19(026):110
Milton JG (2011) The delayed and noisy nervous system: implications for neural control. J Neural Eng 8(065):005
Milton JG, Mackey MC (2000) Neural ensemble coding and statistical periodicity: speculations on the operation of the mind's eye. J Physiol (Paris) 94:489–503
Milton JG, Cabrera JL, Ohira T (2008) Unstable dynamical systems: delays, noise and control. EPL 83: 48001
Milton JG, Ohira T, Cabrera JL, Fraiser RM, Gyorffy JB, Ruizand FK, Strauss MA, Balch EC, Marin PJ, Alexander JL (2009b) Balancing with vibration: a prelude for "drift and act" balance control. PLoS ONE 4:e7427
Mondié S, Dambrine M, Santos O (2002) Approximation of control laws with distributed delays: a necessary condition for stability. Kybernetika 38:541–551
Nijhawan R, Wu S (2009) Compensating time delays with neural predictions: are predictions sensory or motor? Philos Trans R Soc A 367:1063–1078
Otmakhov N, Shirke AM, Malinov R (1993) Measuring the impact of probabilistic transmission on neuronal output. Neuron 10:1101–1111
Palmor ZJ (2000) Time-delay compensation—Smith predictor and its modifications. In: Levine WS (ed) The control handbook. CRC and IEEE Press, Boca Raton, FL, pp 224–237
Patzelt F, Pawelzik KP (2011) Criticality of adaptive control dynamics. Phys Rev Lett 107(238):103
Pau S, Jahn G, Sakreida K, Domin M, Lotze M (2013) Encoding and recall of finger sequences in experienced pianists compared to musically naives: a combined behavioral and functional imaging study. NeuroImage 64:379–387
Schurer F (1948) Zur theorie des balancierens. Math Nachr 1:295–331
Shadlen MN, Newsome WT (1998) The variable discharge of cortical neurons: implications for connectivity, computation and information coding. J Neurosci 18:3870–3896
Shadmehr R, Smith MA, Krakauer JW (2010) Error correction, sensory prediction, and adaptation in motor control. Annu Rev Neurosci 33:89–108
Sieber J, Krauskopf B (2005) Extending the permissible control loop latency for the controlled inverted pendulum. Dyn Syst 20(2):189–199
Skogestad S, Postlewaite I (1996) Multivariable feedback control analysis and design. Wiley, London
Smith OJM (1957) Closer control of loops with dead time. Chem Eng Prog 53(5):217–219
Stanley J, Miall RC (2009) Using predictive motor control processes in a cognitive task: behavioral and neuroanatomical perspectives. Adv Exp Med Biol 629:337–354

Stein G (2003) Respect the unstable. IEEE Control Syst Mag 23:12–25
Stepan G (1989) Retarded dynamical systems. Longman, Harlow
Stepan G (2009) Delay effects in the human sensory system during balancing. Philos Trans R Soc A 367:1195–1212
Suminski AJ, Thach DC, Fagg AH, Hatsopoulos NG (2010) Incorporating feedback from multiple sensory modalities enhances brain–machine interface control. J Neurosci 30:16,777–16,787
Suzuki Y, Nomura T, Casadio M, Morasso P (2012) Intermittent control with ankle, hip, and mixed strategies during quiet standing: a theoretical proposal based on a double inverted pendulum model. J Theor Biol 310:55–79
Todorov E, Jordan MI (2002) Optimal feedback control as a theory of motor coordination. Nat Neurosci 5:1226–1235
Valero-Cuevas FJ, Hoffmann H, Kurse MU, Kutch JJ, Theodorou EA (2009) Computational models for neuromuscular function. IEEE Rev Biomed Eng 2:110–135
Wang QG, Lee TH, Tan KK (1998) Finite spectrum assignment for time-delay systems. Springer, New York
Werner G, Mountcastle VB (1963) The variability of cortical neural activity in a sensory system, and its implications for the central reflection of sensory inputs. J Neurophysiol 26:958–977